

of  $C\alpha 2/5$  and  $C\alpha 3/4$  is unclear. Therefore the mean value  $\delta$  7.91 has been used as reference shift. The  $\delta_{\text{ref}}^{\text{para}}$  values were converted to the final standard values  $\delta_{\text{ref}}^{\text{para}}$  following the Curie law.

**Acknowledgment.** We thank Profs. O. Kahn and B. M. Hoffman for preprints of their publications cited in refs 5 and 2g. Our work has been supported by the Fonds der Chemischen

Industrie and a scholarship (W.S.) of the Technische Universität München.

**Supplementary Material Available:** Calculation of the metal-centered and the ligand-centered dipolar  $^1\text{H}$  and  $^{13}\text{C}$  NMR shifts (6 pages). Ordering information is given on any current masthead page.

## Self-Assembly of Dinuclear Helical and Nonhelical Complexes with Copper(I)

Stéphane Rüttimann,<sup>†</sup> Claude Piguet,<sup>†</sup> Gérald Bernardinelli,<sup>‡</sup> Bernard Bocquet,<sup>†</sup> and Alan F. Williams<sup>\*,†</sup>

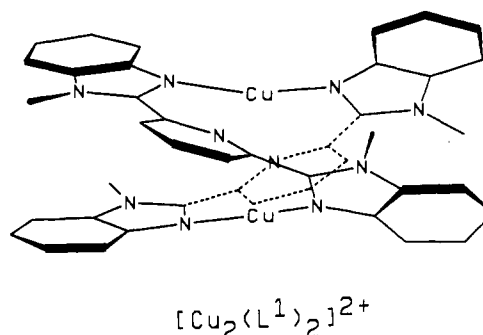
Contribution from the Department of Inorganic, Analytical and Applied Chemistry, and the Laboratory of X-ray Crystallography, University of Geneva, CH 1211 Geneva 4, Switzerland. Received November 1, 1991

**Abstract:** The ligand 1,3-bis(1-methylbenzimidazol-2-yl)benzene (mbzimbe,  $L^3$ ) reacts with copper(I) to give  $[\text{Cu}_2(L^3)_2](\text{ClO}_4)_2$ . The crystal structure of this compound ( $\text{Cu}_2\text{C}_{44}\text{H}_{36}\text{N}_8\text{Cl}_2\text{O}_8$ ,  $a = 13.661$  (1) Å,  $b = 19.829$  (3) Å,  $c = 15.413$  (2) Å, orthorhombic,  $Pbca$ ,  $Z = 4$ ) shows a dinuclear centrosymmetrical nonhelical structure in which each copper is linearly coordinated by a benzimidazole group of each ligand. The complex displays a weak intramolecular stacking interaction between the benzene groups. This complex can be considered as a stereoconformer of the double-helical complex  $[\text{Cu}_2(L^1)_2](\text{ClO}_4)_2$  ( $L^1$ : 2,6-bis(1-methylbenzimidazol-2-yl)pyridine). Conductivity measurements and UV-visible spectra show that the dimeric structures are maintained in solution in polar aprotic solvents.  $^1\text{H}$  NMR measurements show that  $[\text{Cu}_2(L^1)_2]^{2+}$  retains its helical structure in solution. Comparison of helical and nonhelical structures with those formed by Cu(I) with related ligands allows discussion of the factors favoring the formation of self-assembled dinuclear complexes.

### Introduction

The design of complex three-dimensional supramolecular architectures requires the use of selective and efficient self-assembling processes.<sup>1</sup> A feature of self-assembly is the use of elementary modular building blocks which contain sufficient structural information to guide the self-assembly reaction.<sup>2</sup> These reactions may be driven by the formation of specific intra- and intermolecular interactions between units, as is well-known in biological systems, or by the complexation of the modules to a metal ion. The development of new polydentate ligands which give organized supermolecules upon complexation to two or more metal ions is thus a theme of considerable interest in supramolecular chemistry.<sup>1,3</sup> Particular interest has been shown in double-helical structures which may be generated by the complexation of two ligands twisted around metal ions lying on the helical axis. Many such systems have been reported for dimetallic complexes containing cadmium(II),<sup>4</sup> copper(I),<sup>5</sup> copper(II),<sup>6</sup> iron(II),<sup>5</sup> manganese(II),<sup>5</sup> and nickel(II).<sup>7</sup> Planned syntheses of double-helical complexes containing up to five Cu(I) ions have been developed by Lehn and his collaborators,<sup>8</sup> while Dietrich-Buchecker and Sauvage<sup>9</sup> used double-helical complexes with Cu(I) for the synthesis of the first molecular knot. Although most helical complexes with Cu(I) display tetrahedral coordination around the metal ion,<sup>5,8,9</sup> we recently reported<sup>10</sup> a double-helical complex of Cu(I) in which the ligand 2,6-bis(1-methylbenzimidazol-2-yl)pyridine ( $L^1$ , mbzimpy) acts essentially as a bis(monodentate) ligand, giving a quasi-linear coordination of the two copper ions which show, however, a weak interaction with the bridging pyridines. If this interaction is included, the coordination of the copper ions may be considered as a highly distorted tetrahedron.

As an aspect of our general interest in self-assembly reactions, this system offers possibilities for investigating the factors which



favor the self-assembly of polynuclear metal complexes. In particular, we were interested to know if the weak bridging pyridines were essential for the helical twist, and if the double-

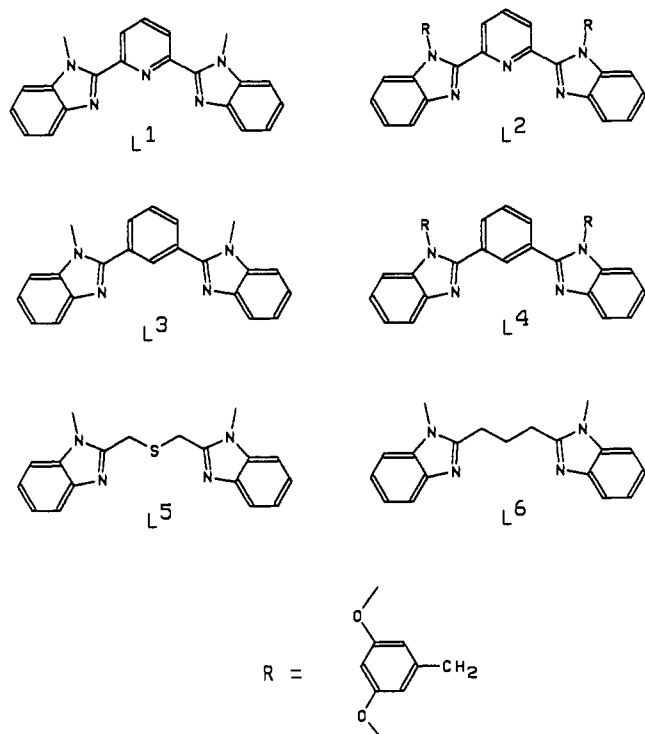
- (1) Lehn, J.-M. *Angew. Chem. Int. Ed. Engl.* **1990**, *29*, 1304.
- (2) Lindsey, J. S. *New J. Chem.* **1991**, *15*, 153.
- (3) Constable, E. C. *Nature* **1990**, *346*, 314.
- (4) Constable, E. C.; Ward, M. D. *J. Am. Chem. Soc.* **1990**, *112*, 1256.
- (5) Constable, E. C.; Ward, M. D.; Tocher, D. A. *J. Chem. Soc., Dalton Trans.* **1991**, 1675.
- (6) Constable, E. C.; Drew, M. G. B.; Ward, M. D. *J. Chem. Soc., Chem. Commun.* **1987**, 1600. Barley, M.; Constable, E. C.; Corr, S. A.; McQueen, R. S.; Nutkins, J. C.; Ward, M. D.; Drew, M. G. B. *J. Chem. Soc., Dalton Trans.* **1988**, 2655.
- (7) Constable, E. C.; Ward, M. D.; Drew, M. G. B.; Forsyth, G. A. *Polyhedron* **1989**, *8*, 2551.
- (8) Lehn, J.-M.; Rigault, A.; Siegel, J.; Harrowfield, J.; Chevrier, B.; Moras, D. *Proc. Natl. Acad. Sci. U.S.A.* **1987**, *84*, 2565. Lehn, J.-M.; Rigault, A. *Angew. Chem., Int. Ed. Engl.* **1988**, *27*, 1095. Koert, U.; Harding, M. M.; Lehn, J.-M. *Nature* **1990**, *346*, 339. Harding, M. M.; Koert, U.; Lehn, J.-M.; Piguet, C.; Rigault, A.; Siegel, J. *Helv. Chim. Acta* **1991**, *74*, 594. Youinou, M.-T.; Ziessel, R.; Lehn, J.-M. *Inorg. Chem.* **1991**, *30*, 2144.
- (9) Sauvage, J.-P. *Acc. Chem. Res.* **1990**, *23*, 319. Dietrich-Buchecker, C. O.; Guilhem, J.; Pascard, C.; Sauvage, J.-P. *Angew. Chem., Int. Ed. Engl.* **1990**, *29*, 1154.
- (10) Piguet, C.; Bernardinelli, G.; Williams, A. F. *Inorg. Chem.* **1989**, *28*, 2920.

\* Address correspondence to this author at the Department of Inorganic, Analytical and Applied Chemistry.

<sup>†</sup> Department of Inorganic, Analytical and Applied Chemistry.

<sup>‡</sup> Laboratory of X-ray Crystallography.

helical structure found in the solid state was maintained in solution. In this paper we show that the replacement of the pyridine in  $L^1$  by a benzene moiety to give the ligand 1,3-bis(1-methylbenzimidazol-2-yl)benzene ( $L^3$ , mbzimbe) allows the synthesis of a Cu(I) complex in which the dinuclearity is maintained, but the helicity is destroyed. Data are presented to show that both helical (with  $L^1$ ) and nonhelical (with  $L^3$ ) structures are maintained in solution in polar aprotic solvents, and an  $^1\text{H}$  NMR probe for helicity is developed. Comparison of these structures with those formed by Cu(I) with related ligands  $L^5$  and  $L^6$  allows identification of some of the factors favoring self-assembly around a metal ion.



## Experimental Section

**Solvents and starting materials** were purchased from Fluka AG (Buchs, Switzerland) and used without further purification, unless otherwise stated. Silica gel (Merck 60, 0.040–0.063 mm) and aluminum oxide (Merck act. II-III, 0.063–0.200 mm) were used for preparative column chromatography.

**Preparation of the Ligands.** The ligand 2,6-bis(1-methylbenzimidazol-2-yl)pyridine ( $L^1$ ) was obtained according to a previously published method.<sup>11</sup> 1,3-Bis(benzimidazol-2-yl)benzene (bzimbe) was prepared from benzene-1,3-dicarboxylic acid and 1,2-diaminobenzene in 66% yield using a modified Phillips reaction<sup>12</sup> and was recrystallized from methanol:  $^1\text{H}$  NMR in DMSO- $d_6$  10.8 (2 H, s, v br), 9.09 (1 H, t,  $J^4 = 1.5$  Hz), 8.27 (2 H, dd,  $J^3 = 8$  Hz,  $J^4 = 1.5$  Hz), 7.72 (1 H, t,  $J^3 = 8$  Hz), 7.63 (4 H, m, [AA'BB']), 7.22 (4 H, m, [AA'BB']); EI-MS 310 ( $M^+$ ). Anal. Calcd for  $C_{20}H_{14}N_4 \cdot 0.5H_2O$ : C, 75.23; H, 4.70; N, 17.55. Found: C, 75.99; H, 4.53; N, 17.34. Bzimbe was alkylated with methyl iodide using the same method as for  $L^1$ <sup>11</sup> to give 1,3-bis(1-methylbenzimidazol-2-yl)benzene ( $L^3$ ) in good yield (77%): mp 179–182 °C;  $^1\text{H}$  NMR in  $CDCl_3$  8.16 (1 H, t,  $J^4 = 1.5$  Hz), 7.95 (2 H, dd,  $J^3 = 8$  Hz,  $J^4 = 1.5$  Hz), 7.85 (2 H, m), 7.73 (1 H, t,  $J^3 = 8$  Hz), 7.44 (2 H, m), 7.36 (4 H, m), 3.94 (6 H, s). Anal. Calcd for  $C_{22}H_{18}N_4$ : C, 78.11; H, 5.33; N, 16.57. Found: C, 77.97; H, 5.27; N, 16.41.

**Preparation of 3,5-Dimethoxybenzyl Bromide.** 3,5-Dimethoxybenzyl alcohol (1.29 g, 6.77 mmol) and 3.104 g (30.6 mmol) of triethylamine were dissolved in dichloromethane (250 mL) at 0 °C under nitrogen. Mesyl chloride (2.64 g, 23 mmol) was slowly added, and the temperature was maintained below 10 °C during the addition. After stirring for 1 h at room temperature, the mixture was washed with 10% ammonium

sulfate (100 mL) and water (100 mL), dried over cellulose, and evaporated to dryness. To the crude mesylate in dry THF (90 mL) was added 3.33 g (38.3 mmol) of anhydrous lithium bromide, and the resulting mixture was stirred at room temperature for 15 h. After evaporation of the solvent, the crude residue was partitioned between dichloromethane (100 mL) and water (100 mL). The aqueous layer was separated and extracted with dichloromethane (100 mL), and the combined organic phases were dried over sodium sulfate and evaporated. The crude product was purified by column chromatography (silica gel,  $CH_2Cl_2$ ) to give 1.54 g (6.66 mmol; yield = 87%) of 3,5-dimethoxybenzyl bromide as a white solid: mp 77–79 °C;  $^1\text{H}$  NMR in  $CDCl_3$  6.54 (2 H, d,  $J^4 = 2$  Hz), 6.39 (1 H, t,  $J^4 = 2$  Hz), 4.43 (2 H, s), 3.79 (6 H, s); EI-MS 232, 230 ( $M^+$ ).

**Preparation of 2,6-Bis[1-(3,5-dimethoxybenzyl)benzimidazol-2-yl]pyridine ( $L^2$ ) and 2,6-Bis[1-(3,5-dimethoxybenzyl)benzimidazol-2-yl]benzene ( $L^4$ ).** 2,6-Bis(benzimidazol-2-yl)pyridine<sup>12</sup> (0.432 g, 1.39 mmol) was reacted with 0.139 g (3.47 mmol) of sodium hydride (60% oil dispersion) in 10 mL of dry DMF at 0 °C. After stirring 1 h at room temperature, 0.802 g (3.47 mmol) of 3,5-dimethoxybenzyl bromide was added, and the resulting solution was stirred for 18 h. The mixture was then poured into water (150 mL), and the precipitate was filtered, dissolved in dichloromethane (50 mL), dried over sodium sulfate, and evaporated to dryness. The crude product was purified by column chromatography ( $Al_2O_3$ ,  $CH_2Cl_2/MeOH$  99:1) and then crystallized from  $CH_2Cl_2$ /hexane to give 0.706 g (1.15 mmol; yield = 83%) of  $L^2$  as white pellets: mp 171–173 °C;  $^1\text{H}$  NMR in  $CDCl_3$  8.39 (2 H, d,  $J^3 = 8$  Hz), 8.02 (1 H, t,  $J^3 = 8$  Hz), 7.8 (2 H, m), 7.2 (6 H, m), 6.27 (2 H, t,  $J^4 = 2$  Hz), 5.97 (4 H, d,  $J^4 = 2$  Hz), 5.54 (4 H, s), 3.53 (12 H, s); EI-MS 611 ( $M^+$ ). Anal. Calcd for  $C_{37}H_{33}N_5O_4$ : C, 72.65; N, 11.45; H, 5.44. Found: C, 72.05; N, 11.28; H, 5.38.

The same procedure was used to prepare 1,3-bis[1-(3,5-dimethoxybenzyl)benzimidazol-2-yl]benzene ( $L^4$ ) from 1,3-bis(benzimidazol-2-yl)benzene (bzimbe) and 3,5-dimethoxybenzyl bromide (yield = 69%):  $^1\text{H}$  NMR in  $CDCl_3$  8.10 (1 H, t,  $J^4 = 1.5$  Hz), 7.85 (2 H, m), 7.82 (2 H, dd,  $J^3 = 8$  Hz,  $J^4 = 1.5$  Hz), 7.56 (1 H, t,  $J^3 = 8$  Hz), 7.3 (6 H, m), 6.53 (2 H, t,  $J^4 = 2$  Hz), 6.19 (4 H, d,  $J^4 = 2$  Hz), 5.32 (4 H, s), 3.64 (12 H, s); EI-MS 610 ( $M^+$ ).

**Preparation of Copper(I) Complexes.** The complex  $[Cu_2(L^1)_2](ClO_4)_2 \cdot H_2O$  was prepared as described previously.<sup>10</sup> The same procedure was used for the synthesis of  $[Cu_2(L^3)_2](ClO_4)_2$  (yield = 85%). Colorless crystals of  $[Cu_2(L^3)_2](ClO_4)_2$  suitable for an X-ray crystal structure determination were obtained by slow evaporation of a concentrated acetonitrile solution:  $^1\text{H}$  NMR in DMSO- $d_6$  8.09 (2 H, s, br), 8.07 (4 H, d,  $J^3 = 7.5$  Hz), 7.95 (4 H, d,  $J^3 = 7.5$  Hz), 7.72 (4 H, d,  $J^3 = 7.5$  Hz), 7.50 (6 H, t,  $J^3 = 7.5$  Hz), 7.42 (4 H, t,  $J^3 = 7.5$  Hz), 3.57 (12 H, s). Anal. Calcd for  $Cu_2C_{44}H_{36}N_8Cl_2O_8$ : Cu, 12.67; C, 52.69; N, 11.17; H, 3.59. Found: Cu, 13.6; C, 52.47; N, 11.07; H, 3.64.

**Preparation of  $[Cu_2(L^2)_2](ClO_4)_2 \cdot H_2O$  and  $[Cu_2(L^4)_2](ClO_4)_2 \cdot 1.5H_2O \cdot 1.5CH_3CN$ .** All manipulations were performed under nitrogen using Schlenk techniques.  $L^2$  (0.1 g, 0.16 mmol) in dichloromethane (10 mL) was added to a solution of 53.5 mg (0.16 mmol) of  $Cu(CH_3CN)_4(ClO_4)_4$ <sup>13</sup> in acetonitrile (15 mL). The resulting red mixture was concentrated to 4 mL under reduced pressure, and ether was allowed to diffuse into the solution for 3 days. The thin orange needles were separated and dried to give 0.112 g (0.072 mmol; yield = 88%) of  $[Cu_2(L^2)_2](ClO_4)_2 \cdot H_2O$ :  $^1\text{H}$  NMR in  $CD_3NO_2$  8.36 (2 H, t,  $J^3 = 8$  Hz), 8.02 (4 H, d,  $J^3 = 8$  Hz), 7.55 (4 H, td,  $J^3 = 7$  Hz,  $J^4 = 1.5$  Hz), 7.48 (4 H, td,  $J^3 = 7$  Hz,  $J^4 = 1.5$  Hz), 7.30 (4 H, dd,  $J^3 = 7$  Hz,  $J^4 = 1.5$  Hz), 7.19 (4 H, dd,  $J^3 = 7$  Hz,  $J^4 = 1.5$  Hz), 6.51 (4 H, t,  $J^4 = 2$  Hz), 6.30 (8 H, d,  $J^4 = 2$  Hz), 5.52 (4 H, d,  $J^2 = 17.5$  Hz), 5.02 (4 H, d,  $J^2 = 17.5$  Hz), 3.76 (24 H, s); FAB-MS 1449 ( $[Cu_2(L^2)_2](ClO_4)_2$ )<sup>+</sup>. Anal. Calcd for  $Cu_2C_{74}H_{66}N_{10}Cl_2O_{16} \cdot H_2O$ : Cu, 8.11; C, 56.71; N, 8.94; H, 4.37. Found: Cu, 8.4; C, 56.59; N, 8.87; H, 4.37.

The same procedure was used for the preparation of the very air-sensitive colorless  $[Cu_2(L^4)_2](ClO_4)_2 \cdot 1.5H_2O \cdot 1.5CH_3CN$ :  $^1\text{H}$  NMR in  $CD_3NO_2$  8.15 (4 H, d,  $J^3 = 7$  Hz), 8.13 (4 H, d,  $J^3 = 8$  Hz), 8.07 (2 H, t,  $J^4 = 1$  Hz), 7.69 (4 H, d,  $J^3 = 7$  Hz), 7.68 (2 H, t,  $J^3 = 8$  Hz), 7.62 (4 H, td,  $J^3 = 7$  Hz,  $J^4 = 1$  Hz), 7.55 (4 H, td,  $J^3 = 7$  Hz,  $J^4 = 1$  Hz), 6.34 (4 H, t,  $J^4 = 2$  Hz), 6.11 (8 H, d,  $J^4 = 2$  Hz), 5.44 (8 H, s), 3.56 (24 H, s); FAB-MS 1447 ( $[Cu_2(L^4)_2](ClO_4)_2$ )<sup>+</sup>. Anal. Calcd for  $Cu_2C_{76}H_{68}N_{10}Cl_2O_{16} \cdot 1.5H_2O \cdot 1.5CH_3CN$ : C, 58.00; N, 8.13; H, 4.65. Found: C, 58.02; N, 8.11; H, 4.66.

**Caution!** Perchlorate salts with organic ligands are potentially explosive and should be handled with the necessary precautions.<sup>14</sup>

**Crystal structure determination of  $[Cu_2(L^3)_2](ClO_4)_2$ :**  $Cu_2C_{44}H_{36}N_8Cl_2O_8$ ,  $M_r = 1002.8$ ,  $\mu = 1.213 \text{ mm}^{-1}$ ,  $F_{000} = 2048$ ,  $d_x = 1.60 \text{ g} \cdot \text{cm}^{-3}$ ;

(11) Piguet, C.; Bocquet, B.; Müller, E.; Williams, A. F. *Helv. Chim. Acta* 1989, 72, 323.

(12) Addison, A. W.; Burke, P. J. *J. Heterocycl. Chem.* 1981, 18, 803. Addison, A. W.; Rao, T. N.; Wahlgren, C. G. *J. Heterocycl. Chem.* 1983, 20, 1481.

(13) Hathaway, B. J.; Holah, D. G.; Postlewaite, J. D. *J. Chem. Soc.* 1961, 3215.

(14) Wolsey, W. C. *J. Chem. Educ.* 1978, 55, A355.

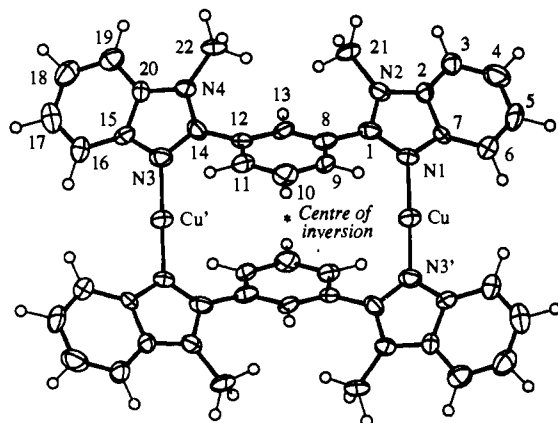


Figure 1. Atomic numbering scheme for  $[\text{Cu}_2(\text{L}^3)_2]^{2+}$ .

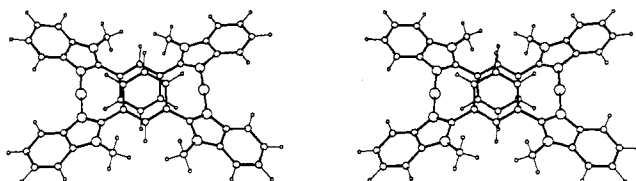


Figure 2. ORTEP<sup>17</sup> stereoscopic view of  $[\text{Cu}_2(\text{L}^3)_2]^{2+}$  perpendicular to the Cu-Cu axis and to the plane of the benzene rings.

orthorhombic,  $Pbca$ ,  $Z = 4$ ,  $a = 13.661$  (1) Å,  $b = 19.829$  (3) Å,  $c = 15.413$  (2) Å,  $V = 4175.1$  (9) Å<sup>3</sup> from 22 reflections ( $22^\circ < 2\theta < 28^\circ$ ); crystal form, colorless prism  $0.10 \times 0.17 \times 0.20$  mm mounted on a quartz fiber. Cell dimensions and intensities were measured at room temperature on a Nonius CAD4 diffractometer with graphite-monochromated  $\text{Mo}[K\alpha]$  radiation,  $\omega$ - $2\theta$  scans, scan width  $1.2^\circ + 0.25 \tan \theta$ , and scan speed  $0.02$ – $0.14^\circ/\text{s}$ ; two reference reflections measured every 60 min showed variations less than  $2.6\sigma(I)$ :  $0 < h < 14$ ;  $0 < k < 21$ ;  $0 < l < 16$ ;  $2^\circ < 2\theta < 46^\circ$ ; 3374 measured reflections, 2898 unique reflections of which 1950 were observable ( $|F_o| > 4\sigma(F_o)$ );  $R_{\text{int}}$  for equivalent reflections 0.017. Data were corrected for Lorentz and polarization effects but not for absorption. The structure was solved by direct methods using MULTAN 87;<sup>15</sup> all other calculations used XTAL<sup>16</sup> system and ORTEP 11<sup>17</sup> programs. Atomic scattering factors and anomalous dispersion terms were taken from ref 18. Full-matrix least-squares refinement based on  $F$  using weight of  $1/\sigma^2(F_o)$  gave final values  $R = 0.071$ ,  $R_w = 0.046$ , and  $S = 2.14$  for 289 variables and 1950 contributing reflections. The mean shift/error on the last cycle was 0.005, and the maximum was 0.025. Hydrogen atoms were placed in calculated positions, and the 32 other atoms were refined with anisotropic displacement parameters. The final Fourier difference synthesis showed a maximum of  $+0.90$  and a minimum of  $-0.70 \text{ e}\text{\AA}^{-3}$ .

**Physical Measurements.** Electronic spectra in the UV-visible range were recorded in solution with Perkin-Elmer Lambda 5 and Perkin-Elmer Lambda 2 spectrophotometers at  $20^\circ\text{C}$  using quartz cells of 1-, 0.1-, and 0.01-cm path length. IR spectra were obtained from KBr pellets with a Perkin-Elmer IR 597 spectrophotometer.  $^1\text{H}$  NMR spectra were recorded on Varian XL 200 (200 MHz) and Bruker AMX 400 (400 MHz) spectrometers. Chemical shifts are given in ppm wrt TMS; abbreviations: s, singlet; d, doublet; t, triplet; m, multiplet. Conductivity measurements were made with a Metrohm E527 Wheatstone bridge connected to a Metrohm EA240 cell ( $f = 0.61 \text{ cm}^{-1}$ ) immersed in a thermostated vessel at  $25^\circ\text{C}$ . DMF was distilled under reduced pressure ( $10^{-2}$  Torr) from  $\text{CaH}_2$ . EI-MS (70 eV) were recorded with VG 7000E and Finnigan 4000 instruments. FAB-MS (positive mode from nitrobenzyl alcohol matrix) were recorded at the Laboratory of Mass Spectrometry of the University of Fribourg (Switzerland). Elemental analyses were performed by Dr. H. Eder of the Microchemical Laboratory of the University of Geneva. Copper was determined by atomic absorption (Pye Unicam SP9) after

(15) Main, P.; Fiske, S. J.; Hull, S. E.; Lessinger, L.; Germain, D.; Declercq, J. P.; Woolfson, M. M. MULTAN 87; Universities of York, England, and Louvain-La-Neuve, Belgium, 1987.

(16) Hall, S. R.; Stewart, J. M. Eds. XTAL 3.0 *User's Manual*; Universities of Western Australia and Maryland, 1989.

(17) Johnson, C. K. ORTEP 11; Report ORNL-5138; Oak Ridge National Laboratory: Oak Ridge, TN, 1976.

(18) *International Tables for X-ray Crystallography*; Kynoch Press: Birmingham, England, 1974; Vol. IV.

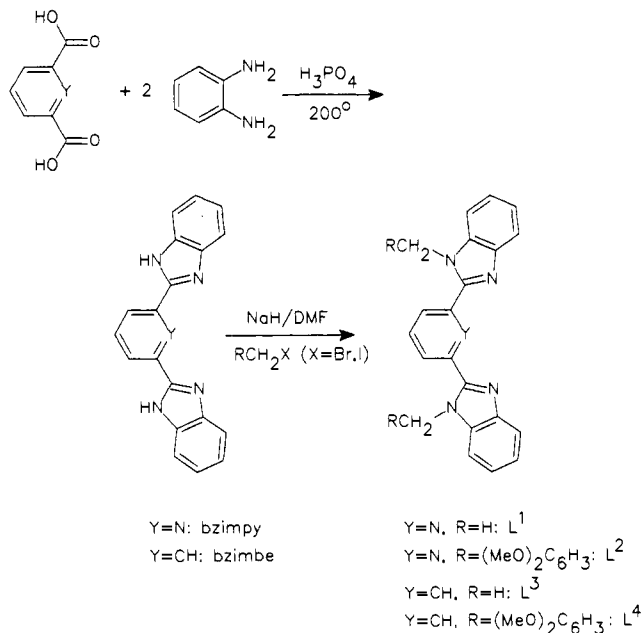
Table I. Selected Bond Distances (Å) and Angles (deg) and Least-Squares Plane Data for  $[\text{Cu}_2(\text{L}^3)_2](\text{ClO}_4)_2$

Cu-N(1)	1.893 (7)	Cu-Cu'	7.140 (2)	
Cu-N(3')	1.888 (7)	N(1)-Cu-N(3')	177.7 (4)	
		deviations, Å		
plane	description	rms	max	
1	benzene, C(8)-C(13)	0.011	0.015	
2	benzimidazole, N(1), N(2)	0.011	0.021	36.7
3	benzimidazole, N(3), N(4)	0.011	0.028	43.7

acidic oxidative mineralization of the complex.

## Results

**Preparation of Compounds.** The ligands 2,6-bis(1-methylbenzimidazol-2-yl)pyridine ( $\text{L}^1$ ), 1,3-bis(1-methylbenzimidazol-2-yl)benzene ( $\text{L}^3$ ), 2,6-bis[1-(3,5-dimethoxybenzyl)benzimidazol-2-yl]pyridine ( $\text{L}^2$ ), and 1,3-bis[1-(3,5-dimethoxybenzyl)benzimidazol-2-yl]benzene ( $\text{L}^4$ ) are obtained in two steps according to a previously described strategy.<sup>11</sup>



The Cu(I) complexes are prepared by mixing ligands  $\text{L}^1$ – $\text{L}^4$  with stoichiometric amounts of  $[\text{Cu}(\text{CH}_3\text{CN})_4]^+$  in acetonitrile or acetonitrile/dichloromethane mixtures. The perchlorate salts can be crystallized easily in good yields either by slow evaporation or by diffusion of ether into the solutions. The complexes of ligands  $\text{L}^1$  and  $\text{L}^2$  with Cu(I) give orange crystals whose elemental analyses are compatible with the formulations  $[\text{Cu}(\text{L}^1)](\text{ClO}_4) \cdot 0.5\text{H}_2\text{O}$  and  $[\text{Cu}(\text{L}^2)](\text{ClO}_4) \cdot 0.5\text{H}_2\text{O}$ . The FAB-MS spectra of  $[\text{Cu}_2(\text{L}^2)_2](\text{ClO}_4)_2 \cdot \text{H}_2\text{O}$  shows the highest significant mass peak at  $m/z = 1449$  with an isotopic distribution corresponding to the species  $[\text{Cu}_2(\text{L}^2)_2(\text{ClO}_4)]^+$ . These results suggest a dimeric formulation for the complexes  $[\text{Cu}_2(\text{L}^1)_2](\text{ClO}_4)_2 \cdot \text{H}_2\text{O}$  and  $[\text{Cu}_2(\text{L}^2)_2](\text{ClO}_4)_2 \cdot \text{H}_2\text{O}$  in agreement with the X-ray crystal structure of the related compound  $[\text{Cu}_2(\text{L}^1)_2](\text{naphthalene-1,5-disulfonate})$ .<sup>10</sup> The complexes of ligands  $\text{L}^3$  and  $\text{L}^4$  with Cu(I) give colorless crystals whose elemental analyses are compatible with the formulations  $[\text{Cu}(\text{L}^3)](\text{ClO}_4)$  and  $[\text{Cu}(\text{L}^4)](\text{ClO}_4) \cdot 0.75\text{H}_2\text{O} \cdot 0.75\text{CH}_3\text{CN}$ . The FAB-MS spectra of  $[\text{Cu}_2(\text{L}^4)_2](\text{ClO}_4)_2 \cdot 1.5\text{H}_2\text{O} \cdot 1.5\text{CH}_3\text{CN}$  shows the highest significant mass peak at  $m/z = 1447$  with an isotopic distribution corresponding to the species  $[\text{Cu}_2(\text{L}^4)_2(\text{ClO}_4)]^+$  which again suggests a dimeric structure for the complexes  $[\text{Cu}_2(\text{L}^3)_2](\text{ClO}_4)_2$  and  $[\text{Cu}_2(\text{L}^4)_2](\text{ClO}_4)_2 \cdot 1.5\text{H}_2\text{O} \cdot 1.5\text{CH}_3\text{CN}$ . The X-ray crystal structure of  $[\text{Cu}_2(\text{L}^3)_2](\text{ClO}_4)_2$  (vide infra) unambiguously confirms its dimeric nature. The IR spectra show characteristic ligand vibrations (C=C, C=N stretching) in the  $1600$ – $1500\text{-cm}^{-1}$  range which are shifted to high energy (about  $5$ – $10 \text{ cm}^{-1}$ ) upon complexation to Cu(I) as previously observed for Cu(II) complexes

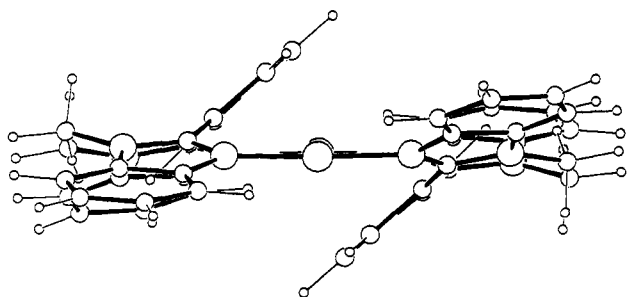
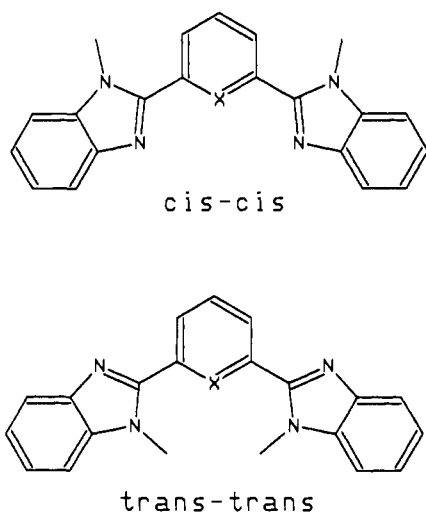


Figure 3. ORTEP<sup>17</sup> view of  $[\text{Cu}_2(\text{L}^3)_2]^{2+}$  along the Cu-Cu axis showing the stacking of the benzene rings.

of  $\text{L}^1$ .<sup>11</sup> The  $\text{ClO}_4^-$  anions all show the two expected symmetrical vibrations ( $1095, 625 \text{ cm}^{-1}$ ) typical of ionic perchlorates.<sup>19</sup> These results strongly suggest that all the complexes are dimeric in the solid state with a dinuclear cation  $[\text{Cu}_2(\text{L})_2]^{2+}$  and two uncoordinated perchlorates.

**X-ray Crystal Structure of  $[\text{Cu}_2(\text{L}^3)_2](\text{ClO}_4)_2$ .** Selected bond distances and angles and selected least-squares plane data are given in Table I. Figure 1 shows the atomic numbering scheme. Figure 2 gives ORTEP<sup>17</sup> stereoview of the complex perpendicular to the Cu-Cu axis, and Figure 3 gives a view along the Cu-Cu axis.

In agreement with the FAB-MS measurements, the crystal structure determination of  $[\text{Cu}_2(\text{L}^3)_2](\text{ClO}_4)_2$  shows it to be composed of a dimeric cation  $[\text{Cu}_2(\text{L}^3)_2]^{2+}$  and two uncoordinated perchlorate anions. The anions have relatively high atomic displacement parameters but otherwise show no features of interest [shortest contact distance with the cation:  $\text{N}(2)-\text{O}(2) = 2.97 \text{ \AA}$ ]. The dimeric cation  $[\text{Cu}_2(\text{L}^3)_2]^{2+}$  is centrosymmetric with the two copper ions occupying equivalent sites and the crystallographically equivalent  $\text{L}^3$  ligands acting as bis(monodentate) ligands. Each copper atom is almost linearly coordinated by two benzimidazole nitrogen atoms, one from each  $\text{L}^3$ , and the N-Cu-N axis lies roughly perpendicular to the Cu-Cu axis. The bond lengths between copper and the bound benzimidazole nitrogen atoms are identical within the precision of the X-ray determination (mean Cu-N bond length:  $1.890 (7) \text{ \AA}$ ), slightly shorter than those observed in  $[\text{Cu}_2(\text{L}^1)_2]^{2+}$ ,  $1.916 \text{ \AA}$ <sup>10</sup> and  $[\text{Cu}(\text{L}^5)]^+$ ,  $1.911 \text{ \AA}$  ( $\text{L}^5 = 2,2'$ -bis(2-*N*-propylbenzimidazolyl)diethyl sulfide, pbzimd);<sup>20</sup> however in both these complexes there is a weak interaction with a third ligating group, either a bridging pyridine<sup>10</sup> or a thioether.<sup>20</sup> In (*N,N,N',N'*-tetra(2'-benzimidazolylmethyl)-1,2-ethanediamine)dicationic copper(I) where the copper is linearly coordinated by two benzimidazoles the average bond distance was  $1.87 \text{ \AA}$ .<sup>21</sup> The



conformation of the ligand  $\text{L}^3$  is related to the trans-trans configuration,<sup>22</sup> but the ligand is twisted about the two interannular bonds giving benzimidazole-phenyl interplane angles of approximately  $40^\circ$ . The two phenyl bridges are stacked coplanar above each other, with an interplane distance of  $3.96 \text{ \AA}$ .

It is interesting to compare the structures of  $[\text{Cu}_2(\text{L}^3)_2]^{2+}$  and  $[\text{Cu}_2(\text{L}^1)_2]^{2+}$ .<sup>10</sup> In  $[\text{Cu}_2(\text{L}^1)_2]^{2+}$  the ligand adopts a cis-cis configuration and twists around the Cu-Cu axis giving a double helical structure with a short Cu-Cu distance  $2.854 (2) \text{ \AA}$  and strong stacking interactions between benzimidazoles in the two chains. The coordination of the copper ions is again essentially linear, with the N-Cu-N axis perpendicular to the helical axis, but there is a weak interaction with the pyridines which act as bridging ligands (av Cu-N(pyridine)  $2.503 \text{ \AA}$ ). In  $[\text{Cu}_2(\text{L}^3)_2]^{2+}$  the trans-trans configuration leads to a much longer Cu-Cu distance ( $7.140 (2) \text{ \AA}$ ), but the Cu-N distances are very similar, and the stacking interaction is now between the bridging phenyl groups, and, judging by the interplane distance, is much weaker. Although the structures appear quite different it is interesting to notice that the only geometric differences lie in the torsion angles for the interannular bonds and those about the Cu-N bonds. If we neglect for an instant the difference between the pyridyl and phenyl bridges between the benzimidazoles, examination of molecular models shows that the two structures may be interconverted without breaking or stretching bonds, but merely by rotation about Cu-N and benzimidazole-pyridine or benzimidazole-benzene bonds. The two structures may thus be regarded as pseudostereoisomers showing helical and nonhelical structures respectively; to our knowledge, this is the first time that such conformers have been fully characterized for coordination compounds.

**Structure in Solution.** The X-ray crystal structures show unambiguously the formation of structured dinuclear assemblies in the solid state, but, if the complexes are to be considered as true examples of controlled self-assembly, it remains essential to show that they are stable in solution and that the double-helical or nonhelical structures are not merely artefacts of the crystallization process. To this end we have studied the conductivity, the UV-visible, and the <sup>1</sup>H NMR spectra in polar aprotic solvents to investigate the nuclearity and the geometry of the complexes in solution.

**1. Conductivity Measurements.** The determination of the equivalent conductivity at one concentration is not sufficient to distinguish between the monomer  $[\text{Cu}(\text{L})]^+$  and the dimer  $[\text{Cu}_2(\text{L})_2]^{2+}$  in solution.<sup>23</sup> However, for strong electrolytes, the changes in equivalent conductivity as a function of the concentration are directly correlated to the electrolyte type of the salt in solution.<sup>23</sup> The Onsager law<sup>23,24</sup> gives  $\Lambda_{\text{eq}} = \Lambda_{\text{eq}}^\circ - A\sqrt{C_{\text{eq}}}$ , and the measurement of  $\Lambda_{\text{eq}}$  at different concentrations  $C_{\text{eq}}$  enables one to determine  $A$  and hence the electrolyte type by comparison with a series of known electrolytes in the same conditions.<sup>25</sup>  $[\text{Cu}_2(\text{L}^1)_2](\text{ClO}_4)_2 \cdot \text{H}_2\text{O}$  and especially  $[\text{Cu}_2(\text{L}^3)_2](\text{ClO}_4)_2$  are poorly soluble in polar aprotic media, but their analogues  $[\text{Cu}_2(\text{L}^2)_2](\text{ClO}_4)_2 \cdot \text{H}_2\text{O}$  and  $[\text{Cu}_2(\text{L}^4)_2](\text{ClO}_4)_2 \cdot 1.5\text{H}_2\text{O} \cdot 1.5\text{CH}_3\text{CN}$ , bearing lipophilic 3,5-dimethoxybenzyl substituents, are readily soluble in solvents such as  $\text{CH}_3\text{CN}$ , DMSO, DMF, and  $\text{CH}_3\text{NO}_2$ . The observed values for the slopes ( $A$ ) of the Onsager law in DMF at  $25^\circ \text{C}$  for  $[\text{Cu}_2(\text{L}^2)_2](\text{ClO}_4)_2 \cdot \text{H}_2\text{O}$  ( $1.54 (5) \times 10^3 [\Omega^{-1} \text{eq}^{-3/2} \text{cm}^2 \text{mol}^{1/2}]$ ) and  $[\text{Cu}_2(\text{L}^4)_2](\text{ClO}_4)_2 \cdot 1.5\text{H}_2\text{O} \cdot 1.5\text{CH}_3\text{CN}$  ( $1.32 (1) \times 10^3 [\Omega^{-1} \text{eq}^{-3/2} \text{cm}^2 \text{mol}^{1/2}]$ ) are typical for 2:1 electrolytes and can be compared with the values obtained for the well-defined 1:1 electrolytes ( $\text{NBu}_4\text{ClO}_4$ ,  $\text{NBu}_4\text{PF}_6$ ) and 2:1 electrolytes ( $\text{Cu}(\text{ClO}_4)_2$ ,  $\text{Cu}(\text{L}^1)(\text{ClO}_4)_2$ <sup>11</sup>) in the same conditions (Table II).

(21) Birker, J. J. M. W. L.; Hendriks, H. M. J.; Reedijk, J. *Inorg. Chim. Acta* **1981**, *55*, L17-L18.

(22) Nakamoto, K. *J. Phys. Chem.* **1960**, *64*, 1420.

(23) Feltham, R. D.; Hayter, R. G. *J. Chem. Soc.* **1964**, 4587.

(24) Boggess, R. K.; Zatzko, D. A. *J. Chem. Educ.* **1975**, *52*, 649.

(25) Dutla, R. L.; Meek, D. W.; Busch, D. H. *Inorg. Chem.* **1970**, *9*, 1215. Sahai, R.; Morgan, L.; Rillema, D. P. *Inorg. Chem.* **1988**, *27*, 3495. Rillema, D. P.; Sahai, R.; Matthews, P.; Edward, A. K.; Shaver, R. J.; Morgan, L. *Inorg. Chem.* **1990**, *29*, 167.

(19) Nakamoto, K. *Infrared and Raman Spectra of Inorganic and Coordination Compounds*, 3rd ed.; John Wiley: New York, Chichester, Brisbane Toronto, 1972; pp 142-154.

(20) Dagdigian, J. V.; McKee, V.; Reed, C. A. *Inorg. Chem.* **1982**, *21*, 1332.

**Table II.** Conductivity Data in DMF at 25 °C<sup>a</sup>

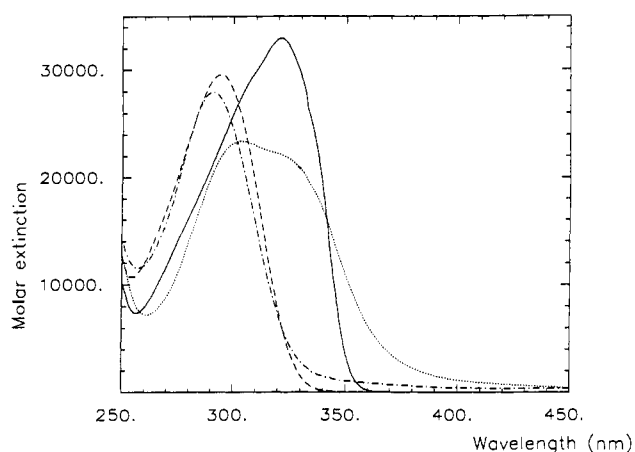
complexes	$\Lambda$ ( $10^{-3}$ M) $\Omega^{-1} \text{ mol}^{-1} \text{ cm}^2$	$\Lambda^0$ $\Omega^{-1} \text{ mol}^{-1} \text{ cm}^2$	slope ( <i>A</i> ) $\Omega^{-1} \text{ cm}^2 \text{ l}^{1/2} \text{ eq}^{-3/2}$	electrolyte
NBu <sub>4</sub> ClO <sub>4</sub>	98 (3)	133 (2)	1098 (37)	1:1
NBu <sub>4</sub> PF <sub>6</sub>	95 (3)	128 (2)	999 (25)	1:1
Cu(ClO <sub>4</sub> ) <sub>2</sub>	224 (5)	320 (5)	1380 (42)	2:1
[Cu(L <sup>1</sup> )](ClO <sub>4</sub> ) <sub>2</sub>	210 (5)	310 (5)	1505 (74)	2:1
[Cu <sub>2</sub> (L <sup>2</sup> ) <sub>2</sub> ](ClO <sub>4</sub> ) <sub>2</sub>	164 (5)	250 (9)	1538 (46)	2:1
[Cu <sub>2</sub> (L <sup>4</sup> ) <sub>2</sub> ](ClO <sub>4</sub> ) <sub>2</sub>	176 (4)	296 (4)	1324 (10)	2:1

<sup>a</sup>  $\Lambda$  ( $10^{-3}$  M), molar conductivity at  $10^{-3}$  M;  $\Lambda^0$ , molar conductivity at infinite dilution; *A*, slope of Onsager law  $\Lambda_{\text{eq}} = \Lambda^0 - A\sqrt{C_{\text{eq}}}$ .

**Table III.** Electronic Spectral Data for the Ligands and Complexes in Propylene Carbonate at 20 °C

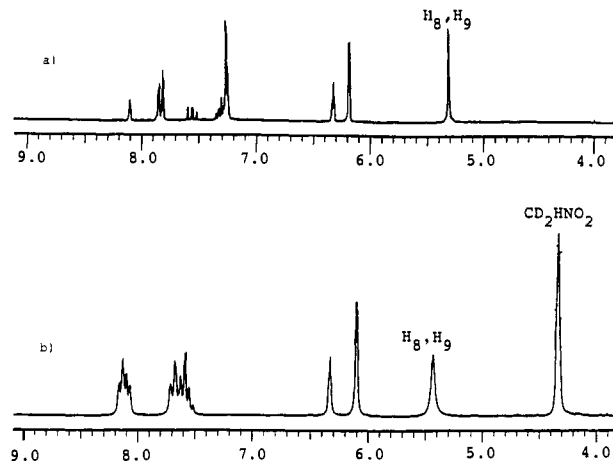
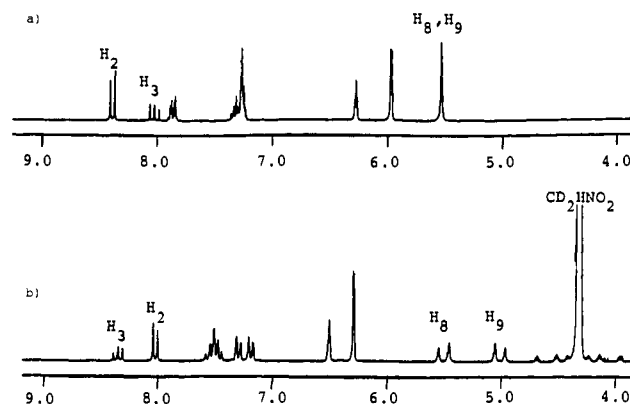
compound	$\pi_1^a \rightarrow \pi^*$	$\pi_1 \rightarrow \pi^*$	$\pi_1^b \rightarrow \pi^*$
L <sup>1</sup>		31 150 (32 000) <sup>a</sup>	
L <sup>2</sup>		30 960 (31 000)	
L <sup>3</sup>		33 800 (29 600)	
[Cu <sub>2</sub> (L <sup>1</sup> ) <sub>2</sub> ](ClO <sub>4</sub> ) <sub>2</sub>	33 000 (46 800)		31 050 (44 300) sh
[Cu <sub>2</sub> (L <sup>2</sup> ) <sub>2</sub> ](ClO <sub>4</sub> ) <sub>2</sub>	32 600 (48 100)		31 250 (46 300) sh
[Cu <sub>2</sub> (L <sup>3</sup> ) <sub>2</sub> ](ClO <sub>4</sub> ) <sub>2</sub>		34 350 (55 800)	

<sup>a</sup> Energies are given for the maximum of the band envelope in  $\text{cm}^{-1}$  and molar absorption coefficient ( $\epsilon$ ) in parentheses in  $\text{M}^{-1} \text{ cm}^{-1}$ ; sh = shoulder.

**Figure 4.** Electronic spectra of the ligands L<sup>1</sup> (—), L<sup>3</sup> (---) and of the complexes [Cu<sub>2</sub>(L<sup>1</sup>)<sub>2</sub>]<sup>2+</sup> (···), and [Cu<sub>2</sub>(L<sup>3</sup>)<sub>2</sub>]<sup>2+</sup> (-·-·).

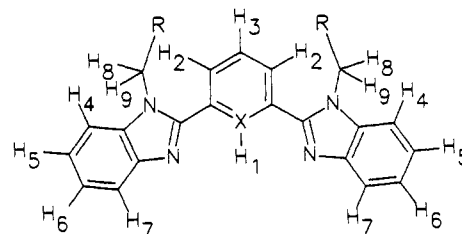
These results imply a dimeric formulation [Cu<sub>2</sub>(L)<sub>2</sub>](ClO<sub>4</sub>)<sub>2</sub> for these complexes and show that the dinuclear structures of the cations [Cu<sub>2</sub>(L)<sub>2</sub>]<sup>2+</sup> are maintained in solution.

**2. UV-Visible Spectra.** The color differences observed in the solid state between complexes of L<sup>1</sup> and L<sup>2</sup> (orange) and those of L<sup>3</sup> and L<sup>4</sup> (colorless) persist in solution. The UV spectra show an intense absorption around 31 000  $\text{cm}^{-1}$  ( $\epsilon = 35\,000\text{--}60\,000 \text{ M}^{-1} \text{ cm}^{-1}$ ) attributed to  $\pi_1 \rightarrow \pi^*$ .<sup>10,11,22</sup> [Cu<sub>2</sub>(L<sup>1</sup>)<sub>2</sub>]<sup>2+</sup> and [Cu<sub>2</sub>(L<sup>2</sup>)<sub>2</sub>]<sup>2+</sup> show the typical splitting of this transition into two components  $\pi_1^a, \pi_1^b \rightarrow \pi^*$  which indicates coordination of the tridentate ligands L<sup>1</sup> or L<sup>2</sup> to Cu(I) in solution.<sup>10,11</sup> In contrast, [Cu<sub>2</sub>(L<sup>3</sup>)<sub>2</sub>]<sup>2+</sup> shows a single unsplit  $\pi \rightarrow \pi^*$  at higher energy whose position and intensity are very similar to that of the free ligand L<sup>3</sup> (Table III, Figure 4). Figure 4 shows that the absorbance for [Cu<sub>2</sub>(L<sup>1</sup>)<sub>2</sub>]<sup>2+</sup> tails off into the visible, whereas [Cu<sub>2</sub>(L<sup>3</sup>)<sub>2</sub>]<sup>2+</sup> shows a sharp cutoff around 330 nm. The origin of this long tail for [Cu<sub>2</sub>(L<sup>1</sup>)<sub>2</sub>]<sup>2+</sup> and [Cu<sub>2</sub>(L<sup>2</sup>)<sub>2</sub>]<sup>2+</sup> is probably a MLCT (Cu(I)  $\rightarrow \pi^*$ ) transition which is expected to fall in the range 25 000–20 000  $\text{cm}^{-1}$  for pseudo-tetrahedral [Cu(I)( $\alpha, \alpha'$ -diimine)<sub>2</sub>] chromophore.<sup>26</sup> This, coupled with the splitting of the  $\pi_1 \rightarrow \pi^*$  into two transitions, suggests strongly that the central pyridine is interacting with the copper as expected for the double helical structure. For linear dicoordinated Cu(I) complexes with heterocyclic nitrogens, the Cu(I)  $\rightarrow \pi^*$  (ligand) MLCT transitions are expected to appear at higher energy<sup>27</sup> (42 000–50 000  $\text{cm}^{-1}$ ) and the spectrum observed for [Cu<sub>2</sub>(L<sup>3</sup>)<sub>2</sub>]<sup>2+</sup> is thus fully compatible with a linear [Cu(I)(ben-

**Figure 5.** <sup>1</sup>H NMR spectrum (200 MHz) of (a) L<sup>4</sup> in CDCl<sub>3</sub> and (b) [Cu<sub>2</sub>(L<sup>4</sup>)<sub>2</sub>]<sup>2+</sup> in CD<sub>3</sub>NO<sub>2</sub>.**Figure 6.** <sup>1</sup>H NMR spectrum (200 MHz) of (a) L<sup>2</sup> in CDCl<sub>3</sub> and (b) [Cu<sub>2</sub>(L<sup>2</sup>)<sub>2</sub>]<sup>2+</sup> in CD<sub>3</sub>NO<sub>2</sub> showing the AB spectrum of H<sub>8</sub> and H<sub>9</sub>.

zimidazole)<sub>2</sub>]<sup>+</sup> chromophore in agreement with the solid-state structure.

**3. NMR Spectra.** The <sup>1</sup>H NMR spectra of the free ligands L<sup>1</sup>–L<sup>4</sup> show two equivalent benzimidazoles giving a complicated multiplet between 7.3 and 7.9 ppm for the protons H<sub>4</sub>–H<sub>7</sub> and a singlet for the methylene group (H<sub>8</sub>, H<sub>9</sub>) or methyl group attached to the benzimidazole nitrogen atoms (Table IV, Figures 5a and 6a). The central aromatic ring (pyridine or benzene) protons give pseudo-first-order spectra, at lower field when the ligand possesses a pyridine nucleus (L<sup>1</sup> and L<sup>2</sup>).



Upon complexation to Cu(I), the <sup>1</sup>H NMR signals of the benzimidazole protons H<sub>4</sub> to H<sub>7</sub>, of ligands L<sup>1</sup>–L<sup>4</sup> are slightly modified, as already described for [Cu<sub>2</sub>(L<sup>1</sup>)<sub>2</sub>]<sup>2+</sup>,<sup>10</sup> to give pseu-

(26) Müller, E.; Piguet, C.; Bernardinelli, G.; Williams, A. F. *Inorg. Chem.* **1986**, *27*, 849. Phifer, C. C.; McMillin, D. R. *Inorg. Chem.* **1986**, *25*, 1329.  
(27) Sorrell, T. N.; Borovik, A. S. *J. Am. Chem. Soc.* **1986**, *108*, 5636.

**Table IV.**  $^1\text{H}$  NMR Shifts (with Respect to TMS) for Ligands  $\text{L}^1\text{--L}^4$  and Complexes in Aprotic Solvents<sup>a</sup>

	solvent	$\text{H}_4\text{--H}_7$	$\text{H}_5\text{--H}_6$	$\text{H}_1$	$\text{H}_2$	$\text{H}_3$	$\text{H}_8\text{--H}_9$
$\text{L}^1$	$\text{CDCl}_3$	7.3–7.9 (m)			8.42	8.05	4.25 (s)
$\text{L}^2$	$\text{CDCl}_3$	7.2–7.9 (m)			8.39	8.02	5.54 (s)
$\text{L}^3$	$\text{CDCl}_3$	7.3–7.9 (m)		8.16	7.95	7.73	3.94 (s)
$\text{L}^4$	$\text{CDCl}_3$	7.2–7.9 (m)		8.10	7.82	7.56	5.32 (s)
$[\text{Cu}_2(\text{L}^1)_2]^{2+}$	$\text{CD}_3\text{NO}_2$	6.94, 7.15	7.30, 7.40		8.35	8.55	3.66 (s)
$[\text{Cu}_2(\text{L}^3)_2]^{2+}$	$\text{DMSO-}d_6$	7.72, 7.95	7.41, 7.50	8.11	8.08	7.50	3.57 (s)
$[\text{Cu}_2(\text{L}^2)_2]^{2+}$	$\text{CD}_3\text{NO}_2$	7.19, 7.30	7.48, 7.55		8.02	8.36	5.02 (d)
							5.52 (d)
$[\text{Cu}_2(\text{L}^4)_2]^{2+}$	$\text{CD}_3\text{NO}_2$	7.69, 8.15	7.55, 7.62	8.07	8.13	7.68	5.44 (s)

<sup>a</sup> Key: s, singlet; d, doublet; m, multiplet.

do-first-order spectra with two triplets ( $\text{H}_5$ ,  $\text{H}_6$ ) and two doublets ( $\text{H}_4$ ,  $\text{H}_7$ ) in the range 6.9–7.9 ppm (Table IV, Figures 5b and 6b). For the complexes  $[\text{Cu}_2(\text{L}^1)_2]^{2+}$  and  $[\text{Cu}_2(\text{L}^2)_2]^{2+}$ , the downfield shift of the  $\text{H}_3$  pyridine signal (0.50 ppm for  $[\text{Cu}_2(\text{L}^1)_2]^{2+}$ , 0.34 ppm for  $[\text{Cu}_2(\text{L}^2)_2]^{2+}$ ) is typical for N-coordination of the pyridine ring<sup>28</sup> confirming the UV-visible results. This parallels the behavior of the pyridinium ion<sup>29</sup> where the equivalent proton moves 1.15 ppm downfield and of a Schiff-base derived from 2,6-diformylpyridine where  $\text{H}_3$  is moved by 0.22 ppm upon complexation to Cu(I).<sup>30</sup> For the phenyl bridged complexes  $[\text{Cu}_2(\text{L}^3)_2]^{2+}$  and  $[\text{Cu}_2(\text{L}^4)_2]^{2+}$ , the aromatic protons  $\text{H}_1\text{--H}_3$  display only small shifts which depend strongly on the solvent used.<sup>31</sup> The equivalence of the two benzimidazole groups for all the complexes implies a symmetry element in the cation  $[\text{Cu}_2(\text{L})_2]^{2+}$  which exists both in the helical structure ( $D_2$  symmetry) and in the nonhelical structure ( $C_{2h}$  symmetry).

To establish definitively the helical or nonhelical nature of the complexes  $[\text{Cu}_2(\text{L}^1)_2]^{2+}$  and  $[\text{Cu}_2(\text{L}^3)_2]^{2+}$  in solution the ligands  $\text{L}^2$  and  $\text{L}^4$  were designed. The addition of the 3,5-dimethoxybenzyl group to the backbone of the ligand gives a  $\text{RCH}_2$  probe which may be used to investigate the  $^1\text{H}$  NMR intramolecular diastereotopic effect.<sup>32</sup> If the complex is chiral then the protons  $\text{H}_8$  and  $\text{H}_9$  will be diastereotopic, and we would therefore expect an AB spin system for these two protons in the double-helical chiral cation  $[\text{Cu}_2(\text{L}^2)_2]^{2+}$  ( $D_2$  symmetry); for the centrosymmetrical cation  $[\text{Cu}_2(\text{L}^4)_2]^{2+}$  ( $C_{2h}$  symmetry) an  $A_2$  spin system is expected. A similar, but intermolecular, effect has already been used by Lehn and his collaborators<sup>8</sup> to show the chirality of their metallo-helicates. However, the intermolecular association with a chiral reagent to produce diastereomers often leads to very small  $^1\text{H}$  NMR splitting due in part to the low stability constants between the partners of the reaction.<sup>8,33</sup> The covalent bond between the diastereotopic probe and the backbone of the ligand for  $\text{L}^2$  and  $\text{L}^4$  should lead to an easily detectable effect in the  $^1\text{H}$  NMR spectra. The 3,5-dimethoxybenzyl group was chosen since the methylene group (in the absence of diastereotopic effects) and the additional aromatic protons give only sharp NMR signals, and the bulky aryl group will enhance the solubility of the ligand and its complexes.

The methylene protons ( $\text{H}_8$ ,  $\text{H}_9$ ) of the 3,5-dimethoxybenzyl probes are indeed enantiotopic in  $[\text{Cu}_2(\text{L}^4)_2]^{2+}$  and display the expected  $A_2$  pattern in the NMR spectrum (Figure 5b) which is compatible with an achiral nonhelical structure for  $[\text{Cu}_2(\text{L}^4)_2]^{2+}$  in solution. Although a fast exchange between chiral structures cannot be completely excluded, we observed no line broadening. On the other hand, the methylene protons ( $\text{H}_8$ ,  $\text{H}_9$ ) of the 3,5-dimethoxybenzyl probes are diastereotopic in compound  $[\text{Cu}_2(\text{L}^2)_2]^{2+}$  and give a well-resolved AB pattern in the NMR spectrum (Figure 6b) which confirms the chiral nature of the cation

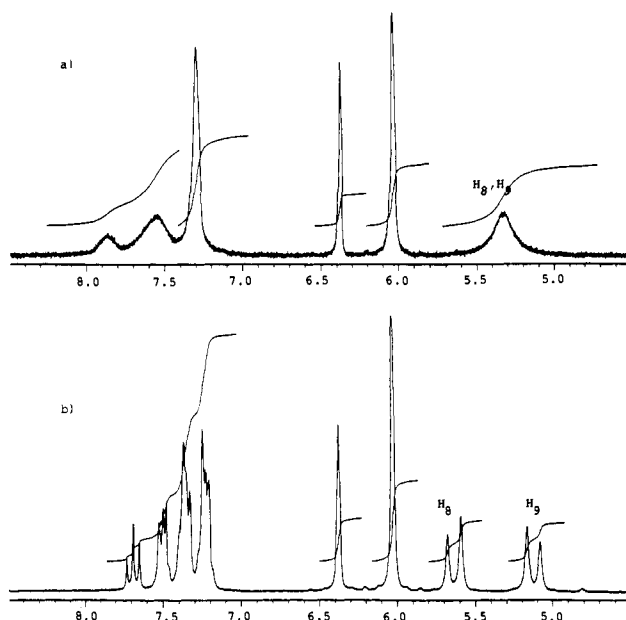


**Figure 7.**  $^1\text{H}$  NMR spectrum 200-MHz of  $[\text{Cu}_2(\text{L}^2)_2]^{2+}$  in  $\text{CD}_3\text{CN}$  at 293 K (a) and 233 K (b).

$[\text{Cu}_2(\text{L}^2)_2]^{2+}$  in solution, as expected from the proposed double-helical structure for this compound.

As observed previously for  $[\text{Cu}_2(\text{L}^1)_2]^{2+}$ ,<sup>10</sup> the NMR signals for compounds  $[\text{Cu}_2(\text{L}^2)_2]^{2+}$  and  $[\text{Cu}_2(\text{L}^4)_2]^{2+}$  at 20 °C in acetonitrile are broad and poorly resolved and display line shapes typical of exchange at a moderate rate on the NMR time scale (Figure 7a). Cooling a solution of  $[\text{Cu}_2(\text{L}^2)_2]^{2+}$  to 233 K leads to a well-resolved spectrum (Figure 7b), very similar to that obtained in nitromethane or DMSO, which can be attributed to the double-helical cation  $[\text{Cu}_2(\text{L}^2)_2]^{2+}$  as the only species present at low temperature. Raising the temperature results in the coalescence of the AB spin system of the methylene protons ( $\text{H}_8\text{--H}_9$ ) into a  $A_2$  spin system strongly indicating the loss of chirality during the exchange mechanism. Previous electrochemical, UV-visible, and NMR studies<sup>10</sup> show that acetonitrile is involved in this exchange process, but several different mechanisms such as monomer  $\leftrightarrow$  dimer, double-helical  $\leftrightarrow$  nonhelical equilibria, or rapid decomplexation of benzimidazole side arms are compatible with the observed results. Such solvent participation has already been reported for the closely related ligand 2,2',6',2''-terpyridyl (terpy) in the complex  $[\text{Cu}(\text{I})(\text{terpy})_2]^+$  where acetonitrile is thought to compete with terpy for complexation to Cu(I).<sup>34</sup>

## Discussion

Having established the stability of the dinuclear species in solution, it is of interest to consider the factors which favor the formation of one or other of these structures. It is also useful to compare the structures with those formed by copper(I) with two other ligands containing two benzimidazoles separated by a three-atom spacer,  $\text{L}^5$ ,<sup>20</sup> and 1,3-bis(1-methylbenzimidazol-2-yl)propane,  $\text{L}^6$ .<sup>35</sup>  $\text{L}^6$  is a simple bidentate ligand which forms

(28) Lavallee, D. K.; Baughman, M. D.; Phillips, M. P. *J. Am. Chem. Soc.* **1977**, *99*, 718.

(29) Abramovitch, R. A.; Davis, J. B. *J. Chem. Soc. B* **1966**, 1137.

(30) Drew, M. G. B.; Lavery, A.; McKee, V.; Nelson, S. M. *J. Chem. Soc., Dalton Trans.* **1985**, 1771.

(31) Rüttimann, S. Ph.D. Thesis No. 2496, Faculty of Sciences, University of Geneva, 1991.

(32) Günther, H. *NMR Spectroscopy*; John Wiley & Sons: Chichester, New York, Brisbane, Toronto, 1980; pp 197–205.

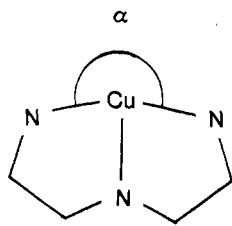
(33) Roza, P. *Angew. Chem. Int. Ed. Engl.* **1978**, *17*, 940.

(34) Crumbliss, A. L.; Poulos, A. T. *Inorg. Chem.* **1975**, *14*, 1529.

a three-coordinate complex  $[\text{Cu}(\text{L}^6)(\text{CH}_3\text{CN})]^+$  with approximately trigonal coordination of the copper. The ligand is sufficiently flexible to allow the formation of an eight-membered chelate ring with a bite angle close to  $120^\circ$ . Although both helical  $[\text{Cu}_2(\text{L}^1)_2]^{2+}$  and nonhelical  $[\text{Cu}_2(\text{L}^3)_2]^{2+}$  dinuclear structures are possible for this ligand, entropy considerations would disfavor formation of the dinuclear complex. The ligand  $\text{L}^3$  is too inflexible to coordinate in the same way as  $\text{L}^6$  without a repulsive interaction between the copper and phenyl hydrogen  $\text{H}_1$ .

$\text{L}^5$  coordinates as a tridentate ligand giving a T-shaped coordination of the copper.<sup>20</sup> The ligand is flexible, and the chain is slightly longer than for  $\text{L}^6$ , and this allows the T-coordination to distort toward trigonal coordination, the N–Cu–N bite angle of  $198^\circ$  being  $18^\circ$  greater than the  $180^\circ$  expected for true T-coordination. Despite this the Cu–S distance is long (2.469 (9) Å), and this was attributed to a misalignment of the sulfur lone pairs with respect to the Cu–S vector;<sup>20</sup> we return to this point below. Molecular models show that  $\text{L}^5$  could equally form a double-helical structure similar to  $[\text{Cu}_2(\text{L}^1)_2]^{2+}$ , with stacking between benzimidazoles and bridging thioether groups between the two coppers; such bridging groups are at least as well established in the literature<sup>36</sup> as bridging pyridine groups,<sup>10,39</sup> and the length of the bridging pyridine–copper bonds ( $\sim 2.5$  Å) in  $[\text{Cu}_2(\text{L}^1)_2]^{2+}$  suggests that the bridging interaction is not particularly strong. Thus, the existence of benzimidazole–benzimidazole stacking and bridging groups between the two coppers does not seem in itself sufficient to lead to the formation of the double helix. We conclude therefore that the formation of the double helix by  $\text{L}^1$  must be due at least partially to the instability of the expected mononuclear complex  $[\text{Cu}(\text{L}^1)]^+$ . This has some precedent in that the closely related ligand terpy does not form a 1:1 mononuclear complex  $[\text{Cu}(\text{terpy})]^+$  but the 1:2 complex  $[\text{Cu}(\text{terpy})_2]^+$  in which the terpy is thought to act as a bidentate ligand, giving a tetrahedral coordination for  $\text{Cu}(\text{I})$ .<sup>34</sup>

Since Cu–N bond distances are very similar for  $\text{Cu}(\text{II})$  and for  $\text{Cu}(\text{I})$ , we may estimate the probable geometry of a  $[\text{Cu}(\text{L}^1)]^+$  complex from data on the  $\text{Cu}(\text{II})$  complexes of  $\text{L}^1$  and its derivatives.<sup>37</sup> In these compounds the  $\text{N}_{\text{benzimidazole}}\text{–Cu–N}_{\text{benzimidazole}}$  angle  $\alpha$  lies in the range  $200\text{--}206^\circ$ , and the three Cu–N bonds may better be described as forming a broad arrow (!) rather than a T. This represents a large distortion from the ideal geometry of a  $\text{CuN}_3$  system ( $\alpha = 120^\circ$ ) and may thus account for the instability of  $[\text{Cu}(\text{L}^1)]^+$ .



The EHMO method<sup>38</sup> has recently been applied to the study of the geometry of the  $[\text{Cu}(\text{NH}_3)_3]^+$  fragment<sup>39</sup> for values of  $\alpha$  between  $70^\circ$  and  $180^\circ$  and was shown to give good agreement with ab initio calculations. The most favorable coordination is with  $\alpha = 120^\circ$ , with only slight destabilization upon increasing  $\alpha$  to  $180^\circ$  (T geometry), although this distortion is accompanied by a weakening of the binding of the central ligand (as observed in  $[\text{Cu}(\text{L}^5)]^+$ ). The authors did not consider the effect of  $\alpha >$

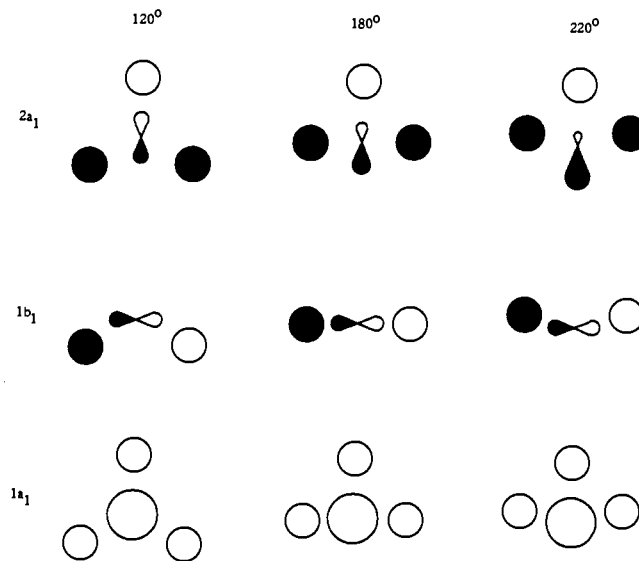


Figure 8. Schematic representation of the Cu–N bonding MO as a function of  $\alpha$ .

$180^\circ$  as is likely for  $\text{L}^1$  and terpy, and so we have carried out such calculations, taking as our model for the ligands three  $\text{sp}^2$  hybridized  $\text{NH}_2$  groups<sup>40</sup> with a constant Cu–N bond distance of 1.95 Å and with  $C_{2v}$  geometry maintained. The results show a significant destabilization of the complex as  $\alpha$  increases above  $180^\circ$ , due to the destabilization of the occupied  $2a_1$  orbital arising from a poorer overlap with the ligand orbitals, which is compounded by the mixing in of the copper 4s orbital in such a way as to direct the  $\text{sp}$  hybrid away from the centroid of the nitrogen atoms. This effect is shown schematically in Figure 8.

Since the rigid nature of mbzimpy and terpy requires them to coordinate with  $\alpha > 180^\circ$  if they are tridentate, it is not surprising that the tridentate geometry is not found in the copper(I) complexes of these ligands. In the case of terpy the formation of a 1:2 complex is preferred to the formation of a double helix, presumably because the stacking interactions seen in  $[\text{Cu}_2(\text{L}^1)_2]^{2+}$  would not exist. We may equally recall that the preference for  $\alpha < 180^\circ$  was also shown by  $[\text{Cu}(\text{L}^5)]^+$  where the value of  $\alpha$  is  $161.8^\circ$ .<sup>20</sup>

Finally we may consider the relative stability of the two conformers of the dinuclear species. The double helix  $[\text{Cu}_2(\text{L}^1)_2]^{2+}$  seems inherently more stable by virtue of the stronger stacking interactions and the presence of the bridging groups, but this structure is not possible for  $[\text{Cu}_2(\text{L}^3)_2]^{2+}$  since the phenyl hydrogens  $\text{H}_1$  would be only 1.5 Å away from the copper atoms. The lower stability of the centrosymmetric structure is shown by the qualitative observation that addition of  $\text{L}^1$  to a colorless solution of  $[\text{Cu}_2(\text{L}^3)_2]^{2+}$  in acetonitrile immediately gives an orange color arising from formation of  $[\text{Cu}_2(\text{L}^1)_2]^{2+}$ ; it is equally shown by the greater reactivity of  $[\text{Cu}_2(\text{L}^3)_2]^{2+}$  toward dioxygen, and this reaction is currently under investigation in our laboratories.

## Conclusions

The structural studies of the complexes  $[\text{Cu}(\text{L}^n)]_m^{m+}$  give insight into the factors favoring self-assembly of supermolecules around metal ions. The ligands used should not be able to bind all their coordination sites to a single metal ion—this may be achieved by a judicious choice of spacer, as in  $\text{L}^3$ , or simply by a mismatch between the geometry of the ligand binding sites and the preferred geometry of the metal ion as with  $\text{L}^1$  and terpy. The role of the spacer is fundamental, as shown by the different structures of the complexes with ligands  $\text{L}^1$ ,  $\text{L}^3$ ,  $\text{L}^5$ , and  $\text{L}^6$  which are all essentially bisbenzimidazoles with different spacers. If the ligand satisfies the above conditions, then self-assembly of dinuclear species is possible; effects such as intramolecular stacking or bridging groups

(35) Bernardinelli, G.; Kübel-Pollak, A.; Rüttimann, S.; Williams, A. F. *Chimica*, in press.

(36) See, for example: Williams, A. F.; Flack, H. D.; Vincent, M. G. *Acta Crystallogr., Sect. B* **1980**, *36*, 1206–1208. Sales, D. L.; Stokes, J.; Woodward, P. *J. Chem. Soc. A* **1969**, 1852–1858.

(37) Sanni, S. B.; Behm, H. J.; Beurskens, P. T.; van Albada, G. A.; Reedijk, J.; Lenstra, A. T. H.; Addison, A. W.; Palaniandavar, M. *J. Chem. Soc., Dalton Trans.* **1988**, 1429–1435. Bernardinelli, G.; Hopfgartner, G.; Williams, A. F. *Acta Crystallogr., Sect. C* **1990**, *46*, 1642–1645.

(38) Hoffmann, R. *J. Chem. Phys.* **1963**, *39*, 1397. Hoffmann, R.; Lipscomb, W. N. *J. Chem. Phys.* **1962**, *37*, 3179; **1962**, *37*, 3489; **1962**, *37*, 2872.

(39) Riehl, J. F.; El-Idrissi Rachidi, I.; Jean, Y.; Pelissier, M. *New J. Chem.* **1991**, *15*, 239–242.

(40) A justification for this is given in the following: Tatsumi, K.; Hoffmann, R. *J. Am. Chem. Soc.* **1981**, *103*, 3328–3341.

may enhance the stability of the resulting complex but are not in themselves sufficient. The dinuclear complexes studied here do not undergo dissociation in polar aprotic solvents, and the incorporation of side chains with potentially diastereotopic protons not only allows the use of  $^1\text{H}$  NMR to determine the presence of helicity in the complexes but also improves the solubility of the ligands. The conditions for self-assembly derived from the detailed study of the complexes presented here should be quite general, and we have recently applied them to the successful synthesis of a dinuclear triple helical coordination compound.<sup>41</sup>

(41) Williams, A. F.; Pigué, C.; Bernardinelli, G. *Angew. Chem., Int. Ed. Engl.* 1991, 30, 1490-1492.

**Acknowledgment.** We gratefully acknowledge support of this research by the Swiss National Science Foundation (Grant No. 21-30139.90).

**Supplementary Material Available:** A full table of bond distances and angles (Table SI) and details of the extended Hückel calculations (Table SIII) (11 pages); full details in the X-ray structure determination of  $[\text{Cu}_2(\text{mbzimbe})_2](\text{ClO}_4)_2$  in the format of the Standard Crystallographic File Structure<sup>42</sup> (Table SII) (15 pages). Ordering information is given on any current masthead page.

(42) Brown, I. D. *Acta Crystallogr., Sect. A* 1985, 41, 399.

## Electrochemistry and Langmuir Trough Studies of $\text{C}_{60}$ and $\text{C}_{70}$ Films

Christophe Jehoulet, Yaw S. Obeng, Yeon-Taik Kim, Feimeng Zhou, and Allen J. Bard\*

Contribution from the Department of Chemistry and Biochemistry, The University of Texas at Austin, Austin, Texas 78712. Received November 26, 1991

**Abstract:** Thin films of the fullerenes  $\text{C}_{60}$  and  $\text{C}_{70}$ , formed by solution casting, were studied by cyclic voltammetry (CV) in MeCN solutions containing quaternary ammonium or alkali-metal salts as supporting electrolytes. The film shows four CV reduction waves and one oxidation wave. The CV behavior for the first reduction, coulometrically equivalent to a one-electron reduction, indicates a large structural reorganization of the film with intercalation of the supporting electrolyte cation and a small amount of dissolution. Upon oxidation of the reduced form, the structure rearranges to form the parent. Similar effects occur for the second reduction/reoxidation process. The size of the cations affects the nature of these CV waves. Scanning electrochemical microscopy (SECM) of the  $\text{C}_{60}$  films indicates that neither the  $\text{C}_{60}$  film nor the completely reduced,  $\text{C}_{60}^-$ , form is a good electronic conductor, while a partially reduced film displays enhanced conductivity. Langmuir trough studies of  $\text{C}_{60}$  and  $\text{C}_{70}$  show the preparation of highly incompressible monolayer and multilayer films at the air/water interface. Mixed films of the fullerenes with the surfactant arachidic acid can also be prepared.

### Introduction

The electrochemical behavior of thin films of the widely investigated fullerenes such as  $\text{C}_{60}$ <sup>1,2</sup> is very different than that of the dissolved species. Several studies of the voltammetric behavior of  $\text{C}_{60}$  and  $\text{C}_{70}$  dissolved in nonpolar solvents such as benzene,  $\text{CH}_2\text{Cl}_2$ , THF, and dichlorobenzene containing quaternary ammonium salts as supporting electrolyte have appeared.<sup>1a,3-6</sup> Generally the reduction is characterized by a series of reversible cyclic voltammetric (CV) waves representing stepwise one-electron reductions to the anion, dianion, etc.; five such waves have been found for  $\text{C}_{60}$  in benzene.<sup>6</sup> The general interpretation of these results is that the reduced forms of  $\text{C}_{60}$  in these solvents and

electrolytes, through the pentaanion, are stable and remain soluble on the CV time scale. The oxidation in benzonitrile occurs at quite positive potentials in a multielectron irreversible CV wave, suggesting a complex oxidation reaction sequence and instability of the radical cation.<sup>6</sup>

We recently reported a preliminary study of the CV behavior of thin ( $\sim 0.1$  to  $1\ \mu\text{m}$ ) films of  $\text{C}_{60}$  cast on various substrates from  $\text{C}_{60}$  solutions.<sup>7</sup> These were carried out in acetonitrile (MeCN) solutions containing quaternary ammonium ( $\text{R}_4\text{N}^+$ ) or alkali-metal salts in which  $\text{C}_{60}$  is not appreciably soluble. Although stepwise reduction was also seen with these films, the behavior was considerably more complicated than that found for the dissolved species. For example, there was a large splitting in potential between the reduction and reoxidation waves for the first electron-transfer reaction, which suggested appreciable reorganization of the film during the redox reaction. We also carried out Langmuir trough studies of  $\text{C}_{60}$ ; these revealed the  $\text{C}_{60}$  films at the air/water interface to be surprisingly stable and highly incompressible.<sup>8</sup>  $\text{C}_{60}$  also formed stable mixed films with eicosanoic (arachidic) acid. In this study we report a more extensive investigation of the electrochemical behavior of  $\text{C}_{60}$  films and the first CV experiments with  $\text{C}_{70}$  films. The use of surface techniques, such as scanning tunneling microscopy (STM), enables us to demonstrate the change of structure of the film during the reduction process. Moreover, it was possible to estimate the relative

(1) (a) Haufler, R. E.; Conceicao, J.; Chibante, L. P. F.; Chai, Y.; Byrne, N. E.; Flanagan, S.; Haley, M. M.; O'Brien, S. C.; Pan, C.; Xiao, Z.; Billups, W. E.; Ciufolini, M. A.; Hauge, R. H.; Margrave, J. L.; Wilson, L. J.; Curl, R. F.; Smalley, R. E. *J. Phys. Chem.* 1990, 94, 8634. (b) Krättschmer, W.; Lamb, L. D.; Fostiropoulos, K.; Huffman, D. R. *Nature* 1990, 347, 354.

(2) (a) Stoddart, J. F. *Angew. Chem. Int. Ed. Engl.* 1991, 30, 70. (b) Diederich, F.; Whetten, R. L. *Angew. Chem. Int. Ed. Engl.* 1991, 30, 678. (c) Kroto, H. W.; Allaf, A. W.; Balm, S. P. *Chem. Rev.* 1991, 91, 1213 and references therein.

(3) Allemand, P.-M.; Koch, A.; Wudl, F.; Rubin, Y.; Diederich, F.; Alvarez, M. M.; Anz, S. J.; Whetten, R. L. *J. Am. Chem. Soc.* 1991, 113, 1050.

(4) Cox, D. M.; Behal, S.; Disko, M.; Gorun, S. M.; Greaney, M.; Hsu, C. S.; Kollin, E. B.; Millar, J.; Robbins, J.; Robbins, W.; Sherwood, R. D.; Tindall, P. *J. Am. Chem. Soc.* 1991, 113, 2940.

(5) Dubois, D.; Kadish, K. M.; Flanagan, S.; Haufler, R. E.; Chibante, L. P. F.; Wilson, L. J. *J. Am. Chem. Soc.* 1991, 113, 4364.

(6) Dubois, D.; Kadish, K. M.; Flanagan, S.; Wilson, L. J. *J. Am. Chem. Soc.* 1991, 113, 7773.

(7) Jehoulet, C.; Bard, A. J.; Wudl, F. *J. Am. Chem. Soc.* 1991, 113, 5456.

(8) Obeng, Y. S.; Bard, A. J. *J. Am. Chem. Soc.* 1991, 113, 6279.